Astrophys. Space Sci. Trans., 5, 49–60, 2009
www.astrophys-space-sci-trans.net/5/49/2009/

Astrophysics and **S**pace Sciences
Trans**a**ctions

Acceleration of the anomalous component of cosmic rays revisited

R. Kallenbach[1,2], K. Bamert[2], and M. Hilchenbach[1]

[1]Max Planck Institute for Solar System Research, 37191 Katlenburg-Lindau, Germany
[2]Physikalisches Institut, University of Bern, 3012 Bern, Switzerland

Received: 24 April 2009 – Revised: 24 June 2009 – Accepted: 28 July 2009 – Published: 13 October 2009

Abstract. In the years 2004 and 2007, the instruments onboard the Voyager 1 and 2 spacecraft delivered unprecedented data on the structure of the solar wind termination shock. This shock has been assumed to be responsible for the acceleration of the anomalous component of cosmic rays from a pick-up ion seed population derived from the interstellar neutral gas penetrating the heliosphere. In expectation of the Voyager observations near the termination shock and in the heliosheath region, detailed models have been developed on the acceleration mechanism for the anomalous cosmic rays and on the structure of the termination shock. Here, an overview on the models on injection mechanisms into first-order Fermi acceleration, stochastic acceleration in the supersonic and subsonic solar wind, shock mediation by suprathermal ions, and on shock reformation by ions reflected at the shock is given. Comparing the results of these models to the Voyager observations, we try to synthesize an updated picture on the acceleration process of the anomalous cosmic rays.

1 Introduction

The anomalous component of cosmic rays (ACRs) originate in the neutral gas of the local interstellar medium (Fisk et al., 1974). This gas penetrates the heliosphere, is ionized by solar radiation or by charge exchange with the solar wind. The resulting ions are then stochastically accelerated in the upstream solar wind and convected outward to the heliosheath. It has long been assumed that the ACRs are mainly accelerated at the solar wind termination shock. After the passage of the Voyager 1 and 2 spacecraft through the termination shock (Burlaga et al., 2008; Decker et al., 2008; Richardson et al., 2008), observations are available that support the view that stochastic acceleration is an important mechanism energizing the ACRs. In fact, the solar wind termination shock as observed by Voyager 1 and 2 is typically too weak to accelerate the ACRs.

In this article, we discuss the physics of the heliospheric interface region in the context of recent observational data. In Sect. 2, we show that models on the processes of shock reformation (Scholer et al., 2003) and shock mediation (Alexashov et al., 2004) have well predicted the observed structure of the termination shock region. Recently, Fahr and Chalov (2008) have explained the observed supercritical termination shock transition by a straightforward analytical two-fluid model.

However, observed spectra of ACRs and termination shock energetic particles (TSPs) are inconsistent with the assumption that first-order Fermi acceleration is the only process energizing these particles (Sect. 3). In Sect. 4, we give an integrated picture on the evolution of turbulence and suprathermal ion populations with heliocentric distance. The predicted flux and spectra of ACRs resulting from stochastic acceleration in the upstream solar wind and in the heliosheath as the main energizing process are consistent with observations by the Voyager 1 and 2 spacecraft and with observations of energetic neutral atoms (ENAs) near Earth's orbit by several instruments.

2 Structure of the termination shock region

Most information on the bulk plasma properties in the heliospheric interface region has been gained when the Voyager 2 spacecraft has passed the solar wind termination shock in 2007. At this location the termination shock is a quasi-perpendicular supercritical shock that undergoes reformation (Burlaga et al., 2008; Decker et al., 2008; Richardson et al., 2008). The downstream thermal protons are still supersonic

Correspondence to: R. Kallenbach
(kallenbach@mps.mpg.de)

Published by Copernicus Publications on behalf of the Arbeitsgemeinschaft Extraterrestrische Forschung e.V.

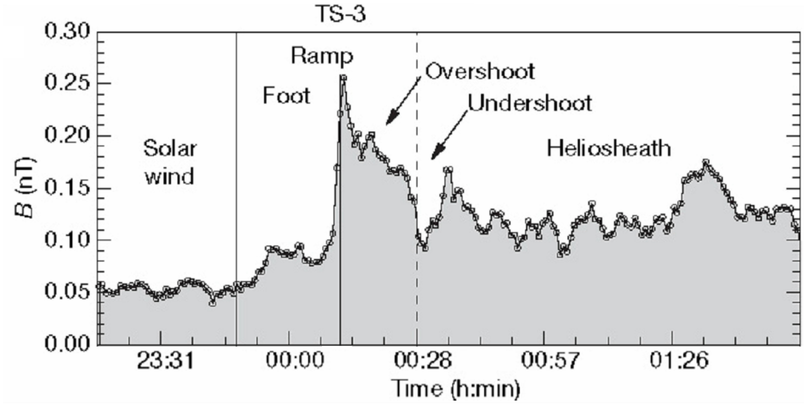

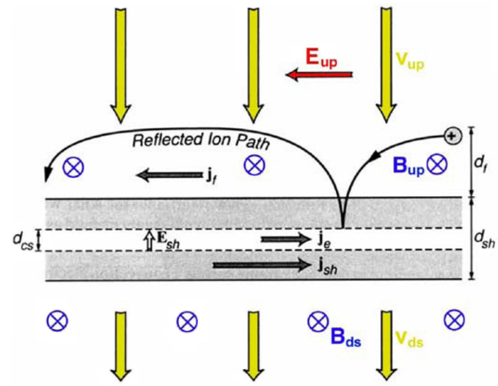

Fig. 1. (left panel) Snapshot of the structure of the solar wind termination shock observed by the Voyager 2 magnetometer (Burlaga et al., 2008). The shock foot has been passed in 23 min, while the shock ramp has been passed in 1.5 min by the Voyager 2 spacecraft which cruises at 15.5 km/s. **(right panel)** Shock foot and overshoot correspond to expectations from basic space plasma physics (Baumjohann and Treumann, 1996)

because the dissipated energy is mainly transferred into the suprathermal ion population. The magnetic micro-structure of the termination shock is characterized by a pronounced shock foot and an overshoot, while on larger scales a strong shock precursor has been identified.

2.1 Supercritical subshock transition

A supercritical termination shock transition has already been discussed by Lee (1998). It also has been treated in full-particle numerical simulations by Scholer et al. (2003) which are based on more general shock structure simulations by Lembège and Savoini (1992). Supercriticality follows from a much stronger pick-up ion heating rather than solar wind proton heating at the shock. In the two-fluid model of Fahr and Chalov (2008), the total pressure balance at the termination shock transition includes the dynamic solar wind pressure, the thermal pressure of the bulk solar wind protons, and the pressure of the pick-up ions caused by their highly suprathermal velocity distribution (Vasyliunas and Siscoe, 1976). The magnetic moment $\mu = mv_\perp^2/(2B)$ (m: ion mass, B: ambient magnetic field strength, $v_\perp$: ion velocity perpendicular to the ambient magnetic field) of suprathermal pick-up ions is much higher than for thermal protons. If this magnetic moment is conserved when passing the magnetic field increase at the shock, the pick-up ions are heated much stronger than the solar wind protons. Consequently, the bulk solar wind protons remain rather cool in the downstream heliosheath plasma and, in fact, their flow can remain supersonic. Upstream and downstream Mach numbers at the termination shock transition can well be reconciled with Voyager 2 data if it is assumed that the pitch-angle scattering of the pick-up ions is strong in the downstream heliosheath plasma but weak in the upstream supersonic solar wind plasma.

2.2 Magnetic micro-structure

It has also been pointed out by Lee et al. (2009) that pick-up ions dominate the dissipation process of upstream bulk energy in the supercritical termination shock rather than Joule heating of electrons. In addition to the heating of pick-up ions by the conservation of their magnetic moment, the reflection process at the electric potential of the quasi-perpendicular termination shock contributes to the heating of pick-up ions. Figure 1 shows the shock foot due to reflected pick-up ions causing a drift current density $\mathbf{j}_f$ and the overshoot due to the shock current $\mathbf{j}_{sh}$ in Voyager 2 data (left panel) and, for illustration, in a sketch (right panel) taken from Baumjohann and Treumann (1996). The amount of magnetic field change in the shock foot is a significant fraction of the magnetic field change across the central steep shock ramp. This suggests that a significant fraction of upstream ions are reflected at the cross-shock electric field. Protons with the velocity of the bulk solar wind, however, have a low probability to be reflected at the cross-shock potential (e.g. Lee et al., 1996; Kallenbach et al., 2005a), while a much larger fraction of pick-up protons of interstellar origin are reflected at a quasi-perpendicular shock. These pick-up ions have a shell-like velocity distribution (Vasyliunas and Siscoe, 1976), where the shell is centered at the solar wind bulk velocity and has a radius of approximately solar wind bulk speed. Therefore, a large fraction of pick-up ions has a small relative speed with respect to the termination shock and is likely to be reflected because the cross-shock potential approximately corresponds to the kinetic energy per charge of the bulk solar wind protons. The shock foot (Fig. 1) has a size of about 20 000 km which is somewhat smaller than the gyro-radius of protons traveling with about 300 km/s in a magnetic field of about 0.05 nT i.e. 60 000 km – as expected.

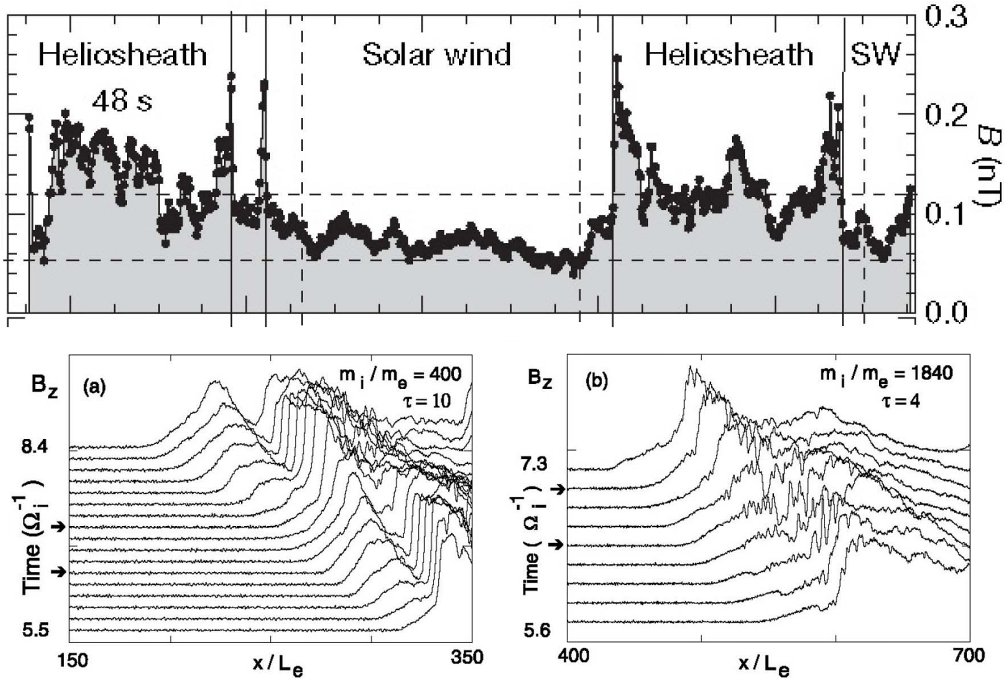

Fig. 2. (upper panel) Magnetic field data of Voyager 2 give evidence for the process of reformation of the termination shock (Burlaga et al., 2008) on a time scale similar to the inverse proton gyro-frequency of order 1000 s. Minimum shock ramp scale sizes are in the range of one to few 1000 km. **(lower panel)** Simulation results by Scholer et al. (2003) predicting the reformation of the termination shock due to pick-up ion pile-up upstream of the shock. Present computer resources still prohibit a completely realistic simulation with a correct ion-to-electron mass ratio $m_\mathrm{i}/m_\mathrm{e}$ and at the same time an appropriate ratio $\sqrt{\tau} = \omega_\mathrm{pe}/\Omega_\mathrm{ce}$ of the electron plasma frequency to the electron cyclotron frequency in the termination shock region. The shock normal angle has been chosen to be 87°.

2.3 Shock reformation

Burlaga et al. (2008) have found that the termination shock undergoes reformation on a time scale roughly corresponding to the inverse proton gyro-frequency (Fig. 2). This phenomenon has been predicted, and numerically simulated by Scholer et al. (2003) as well as analyzed analytically by Matsukiyo and Scholer (2003). The process of shock reformation has consequences for the steepness and the steadiness of the main shock ramp. While minimum shock ramp scale sizes are predicted to be as small as a few electron inertial lengths, this steep ramp can only be maintained over short periods of time. Possible scale sizes for the termination shock ramp are the ion (proton) inertial length, which is of order 10 000 km, the electron inertial length, which is of order 300 km, or the proton gyro-radius, which is of order 60 000 km. The data of Fig. 2 generally support the simulations by Scholer et al. (2003) which predict that the ramp scale size is somewhere between the electron and proton inertial range, and that part of the potential drop occurs at times across the foot, and part of the potential ($\sim 40\%$) occurs over a few ($\sim 4L_\mathrm{e}$) electron inertial lengths in the steepened-up ramp. The exact ramp scale size is hard to determine from a single spacecraft measurement because the relative speed of the termination shock with respect to the Voyager 2 spacecraft is not known.

The changing ramp scale size of the reforming quasi-perpendicular termination shock presumably reduces the injection efficiency of pick-up ions into first-order Fermi acceleration. Injection thresholds at the termination shock may range up to a few hundred keV/amu (compare Fig. 5 below). Such high injection thresholds could be surpassed by coherent shock surfing (Sagdeev, 1966; Lee et al., 1996; Zank et al., 1996a; le Roux et al., 2000), if the termination shock ramp were a steady damped solitary magnetosonic wave with a ramp scale size of about one electron inertial length (Tidman and Krall, 1971). As this is not the case, the efficiency of injecting ions by the the process of acceleration during multiple reflection at the potential of the termination shock may be limited even at locations where the shock is rather quasi-perpendicular.

2.4 Shock mediation

At larger spatial scales, suprathermal ions also play a major role in determining the structure of the termination shock. Voyager 2 observations indicate that shock mediation occurs due to the pressure of suprathermal ions i.e. the ACRs and the termination shock energetic particles (TSPs). This pressure can only be transferred to the upstream bulk plasma over a scale corresponding to the approximate mean free path of the

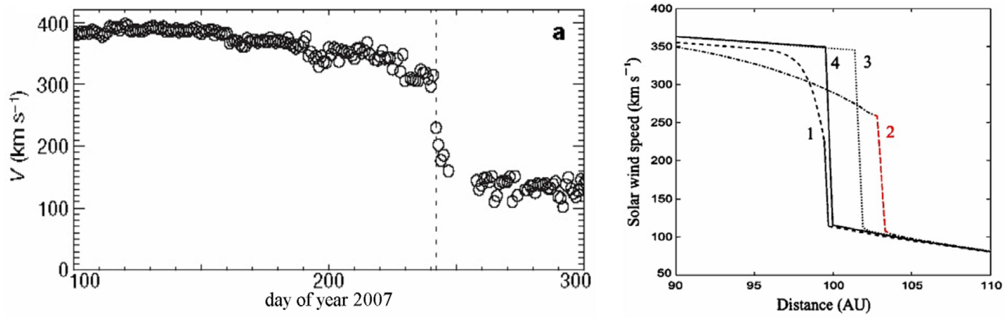

Fig. 3. (left panel) Voyager 2 data on the solar wind bulk speed in the termination shock region (Richardson et al., 2008). **(right panel)** Theoretical predictions by Alexashov et al. (2004) for different mean free paths in the heliosheath, where solution 2 reproduces the observed slow-down. This solution assumes $\lambda_\parallel \approx 0.5$ AU as energy-averaged mean free path in the heliosheath. Solutions 1 and 3 refer to mean free paths of 0.05 AU and 5 AU respectively, but clearly do not reproduce data. Solution 4 represents the solution assuming absence of suprathermal particles.

ACRs and TSPs. The observed shock precursor scale size is about 0.7 AU (Fig. 3, left panel). At shock-normal angles of about 80°, this corresponds to energy-averaged parallel mean free paths of $\lambda_\parallel \approx 4$ AU in the upstream solar wind plasma. As will be shown in more detail in Sect. 4.1, this mean free path is consistent with models on the evolution of turbulent power with heliocentric distance (Kallenbach et al., 2006; Zank et al., 2006).

The amount of slow-down of the upstream solar wind is consistent with simulations by Alexashov et al. (2004). In their solution 2 (Fig. 3, right panel) they assume $\lambda_\parallel \approx 0.5$ AU as energy-averaged mean free path in the heliosheath. Mean free paths of less than 1 AU are also roughly consistent with the spatial gradients of suprathermal ions in the heliosheath (Stone et al., 2005; Kallenbach et al., 2006). Such short mean free paths are sufficient to confine shock-accelerated ions in the heliosheath with a pressure that is comparable to the ambient pressure of the Local Interstellar Medium (Fig. 4).

3 Is the source of the anomalous cosmic rays at the solar wind termination shock?

Although the simulations by Alexashov et al. (2004) predict the correct order of magnitude of the slow-down of the upstream solar wind, they do not give a clear handle to decide whether first-order Fermi acceleration at the termination shock is sufficient to energize the ACRs. Recently, Kallenbach et al. (2006); Moraal et al. (2006); Zhang (2006); Ferreira et al. (2007) performed model calculations solving the Parker equation in various degree of complexity including momentum diffusion. All of them showed that ACR observations at the shock could be explained by adding stochastic acceleration and heating of ACRs or that first-order Fermi acceleration is not required at all (Kallenbach et al., 2006). Fahr (2002) has found analytical solutions to describe the process of transfer of energy from the pick-up ion population to turbulent waves in the solar wind which in turn dissipate their energy into the bulk solar wind protons. The relative importance of first-order and second-order Fermi acceleration all over the heliosphere still remains to be evaluated in more detail from data to be compared to theoretical models. Continuous stochastic acceleration in the inner heliosheath by compressional fluctuations (Bykov and Toptygin, 1981) should reduce the decrease of ACR pressure as a function of heliocentric distance or could even lead to an increase of ACR pressure towards the heliopause. Therefore, ACR pressure profiles in the heliosheath may indicate whether first-order Fermi acceleration at the termination shock is the main process that energizes the ACRs or whether second-order Fermi (stochastic) acceleration is the most important process.

3.1 Injection and acceleration efficiencies at the termination shock

It is clear that the solar wind termination shock can only be the source of the ACRs if it is an efficient ion accelerator. There are simple arguments against this hypothesis. First of all, the reforming termination shock is in average a very weak shock with compression ratios ranging between 1.5 and 2.5. However, the TSP spectra at the location where Voyager 2 passed the termination shock are rather hard and would require a shock compression ratio of about 3 (Decker et al., 2008). The observed spectral index is -1.25 which is close but not identical to the spectral index of -1.5 observed for most of the ubiquitous suprathermal tails (Gloeckler, 2003) presumably created by stochastic acceleration in compressional fluctuations. The observations of Voyager 1 also support the hypothesis that the termination shock is not the source of the ACRs.

McComas and Schwadron (2006); Chalov and Fahr (2000); Fahr et al. (2008); Verscharen and Fahr (2008); Fahr

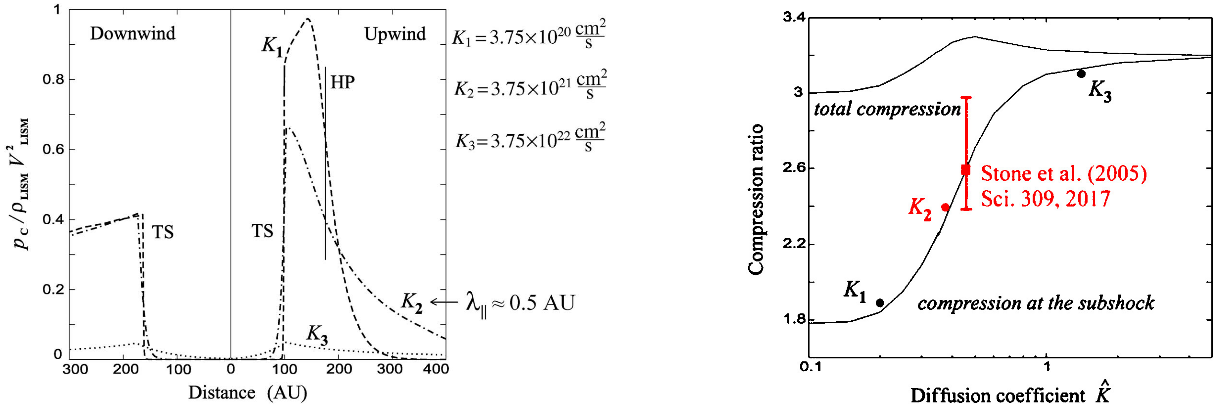

Fig. 4. (left panel) Pressure build-up of suprathermal ions in the heliosheath for different energy-averaged diffusion parameters. **(right panel)** Reduction of the solar wind termination subshock compression ratio due to the mediation by suprathermal ions (Alexashov et al., 2004).

and Verscharen (2008) suggest alternative scenarios where ACR injection does not pre-dominantly occur at locations of quasi-perpendicular shock geometry such as those passed by Voyager 1 and 2 but at locations of quasi-parallel shock geometry. Lowest shock normal angles may be found at high heliolatitudes. However, at high heliolatitudes suprathermal ion tails are rather weak during solar activity minimum so that there are no strong seed populations for injection into first-order Fermi acceleration. Injection and acceleration may be more efficient in the flanks of the heliosphere where the termination shock tends more and more to be an inclined or even quasi-parallel shock. Unfortunately, observations are not available yet from such regions. Scherer and Fahr (2009) also discuss increased injection efficiencies at locations of the termination shock where the sector boundaries of the heliospheric magnetic field influence the termination shock geometry.

However, there are also arguments against these scenarios to apply. Standard models predict that the injection threshold into first-order Fermi acceleration is still rather large at any shock-normal angle down to 60 or 50° (Fig. 5). According to Giacalone and Jokipii (1999), the threshold for injection of suprathermal ions into the first-order Fermi acceleration process at a shock with upstream solar wind speed V_1 in the shock frame is

$$v_{\mathrm{inj}} = 3V_1 \sqrt{1 + \frac{\left(\frac{\kappa_{\mathrm{A}}}{\kappa_\parallel}\right)^2 \sin^2\Psi + \left(1 - \frac{\kappa_\perp}{\kappa_\parallel}\right)^2 \sin^2\Psi\cos^2\Psi}{\left[\left(\kappa_\perp/\kappa_\parallel\right)\sin^2\Psi + \cos^2\Psi\right]^2}}. \quad (1)$$

Here, $\kappa_\parallel$ and $\kappa_\perp$ are the spatial diffusion parameters parallel and perpendicular to the magnetic field, and κ_{A} is the anti-symmetric component of the diffusion tensor. See Appendix A of Kallenbach et al. (2006) for a derivation of Eq. (1) and for the expressions for $\kappa_\perp$ and κ_{A} for the case in which the gyroradius r_{g} of the ion at speed v is small compared

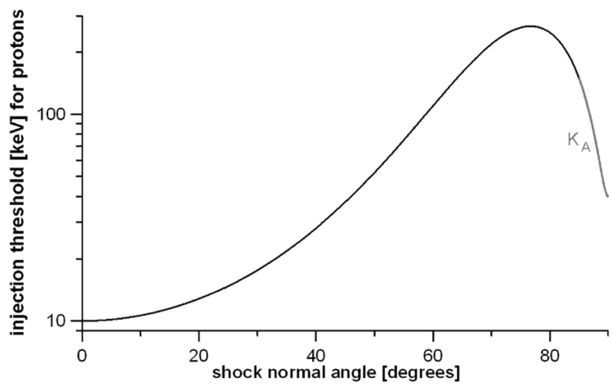

Fig. 5. Injection threshold into first-order Fermi acceleration of protons as a function of the solar wind termination shock normal angle.

to the parallel mean free path $\lambda_\parallel$. Figure 5 shows the injection threshold for protons as a function of the shock normal angle Ψ, based on the turbulence levels that are consistent with observations (Figs. 3 and 4) and on the assumption $\kappa_\perp/\kappa_\parallel \approx r_{\mathrm{g}}^2/\lambda_\parallel^2$. Including the 'meandering' of magnetic field lines or other more refined mechanisms usually leads to a larger ratio $\kappa_\perp/\kappa_\parallel$ and, hence, lowers the injection threshold at quasi-perpendicular shocks. Furthermore, it follows from the solution of an Ito-stochastic differential equation system for the pick-up ion phase-space transport (Chalov and Fahr, 2000) that injection at quasi-perpendicular shocks can be quite efficient. On the other hand, Verscharen and Fahr (2008); Fahr and Verscharen (2008) discuss refined scenarios which predict increased injection efficiency at locations of quasi-parallel termination shock locations. Overall, the injection efficiency may not vary too much for different locations of the heliospheric interface region because variations of the solar wind ram pressure and magnetic field structure cause 'local' variations in the shock normal angle anyway.

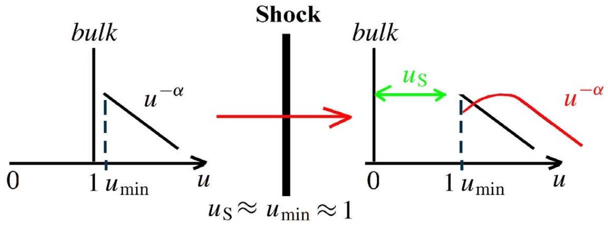

Fig. 6. Schematic showing the characteristics of the transmission of power-law suprathermal tails through a shock potential. Detailed numerical simulations on the post-shock pick-up ion energy distribution can be found in Chalov and Fahr (2000).

3.2 What determines the composition of anomalous cosmic rays?

A further argument against the scenario of ACRs being the result of first-order Fermi acceleration at the termination shock is the ACR composition i.e. the enrichment of heavy masses (Stone et al., 2005). In fact, Stone et al. (2005) introduced the new term TSPs instead of the ACRs for the suprathermal ions near the termination shock because the TSPs have different composition than those typically observed in ACRs inside the heliosphere. Possibly, these abundances can be explained by the following scenario: (1) TSPs are ions that are multiply reflected at the shock potential (le Roux et al., 2000) and injected into first-order Fermi acceleration, which has an injection threshold as shown in Fig. 5. The TSPs do not undergo mass-per-charge (A/Q) fractionation because shock surfing, or acceleration of ions during multiple reflections, respectively, is a process independent of A/Q. (2) ACRs are suprathermal ions directly transmitted through the electric potential of the termination shock, but not returned to the shock for first-order Fermi acceleration. These ions undergo stochastic acceleration in the heliosheath as discussed in more detail in Sect. 4. The transmission through the termination shock potential prefers high A/Q species in concordance with ACR abundances. (3) A fraction of the reflected ions are thermalized into the bulk plasma of the heliosheath. Low A/Q species are preferentially thermalized. This scenario would match observations. For instance, the H/He ratio is about 10 for TSPs and about 5 for ACRs (Stone et al., 2005).

This 'transmission' scenario is quite simple, but can be explained in some more detail as follows: Three populations approach the termination shock from the upstream solar wind: (1) the bulk solar wind ions idealized as a pencil beam $f_{\text{bulk}} \propto \delta\,(u-1, \mu-1)$ (μ: cosine of the pitch angle), (2) the freshly ionized pick-up ions in a shell distribution $q\,(u) \propto \delta\,(u-1)$, and (3) the suprathermal tails $f_{\text{ST}} \propto u^{-\alpha}$ for $u > u_{\text{min}}$. The suprathermal tails at the termination shock presumably reach down to almost $u_{\text{min}} \approx 1$ ($u = v/V_{\text{up}}$ with V_{up} the upstream solar wind speed) because the speeds of the waves causing these tails are much smaller than the speed $U_{\text{up}} = 1$ of the supersonic bulk solar wind. In a very idealized picture, the cross-shock potential is characterized by $u_S \approx 1$, which stops the bulk protons to zero speed. Of course, in reality u_S is less than unity because the downstream plasma does not have exactly zero speed.

According to Kallenbach et al. (2005a), the transmission of ions of mass-per-charge ratio $\mathcal{R} = A/Q$ of population (3) through the shock (excluding the effect of the conservation of the magnetic moment) is

$$T_{S;\mathcal{R}} = \frac{\alpha-1}{2}\left(\frac{u_S}{\sqrt{\mathcal{R}}u_{\text{min}}}\right)^{\alpha-3}\left(1-\frac{u_S^2}{\mathcal{R}u^2}\right). \quad (2)$$

This transmission function is illustrated in Fig. 6. For large A/Q the transmitted phase space density is similar to a power law extending down to $u = u_S\sqrt{Q/A}$ with the same spectral index as the upstream ion distribution, but with lower phase space density than the upstream ions at high u. Therefore, species with large A/Q have little chance to be injected into first-order Fermi acceleration. The species with low A/Q have a larger chance to gain energy at the shock during multiple reflections. The phase space density of the downstream ion distribution at high u is larger than that of the upstream ions. These ions have a good chance to be injected into the first-order Fermi process at the termination shock. However, at small u, suprathermal ions are "missing", and in fact, a significant fraction of the ions with low A/Q may actually be thermalized into the bulk plasma. Therefore, suprathermal ions with low A/Q have a large chance either to undergo shock acceleration or to thermalize in the bulk, while suprathermal ions with large A/Q are mainly transmitted through the shock and subsequently undergo further stochastic acceleration in the heliosheath. If stochastic acceleration occurs by compressional fluctuations, no more A/Q fractionation is expected in the heliosheath.

4 Stochastic acceleration of anomalous cosmic rays

If the ACRs are not accelerated by first-order Fermi acceleration at the termination shock, one natural alternative scenario is stochastic acceleration all over the heliosphere, in particular in the inner heliosheath. This scenario requires turbulence levels which are sufficiently high so that stochastic acceleration is more effective than adiabatic cooling while the suprathermal ions are convected in the solar wind.

4.1 Evolution of turbulence with heliocentric distance

Already before the Voyager 2 observations, Zank et al. (2006) and Kallenbach et al. (2006) have modeled the evolution of the mean free path of energetic particles over heliocentric distance which requires modeling of solar wind turbulence over heliocentric distance. The authors have concentrated on the slow solar wind where the main sources of compressional turbulence are the stream-stream interaction, the decay of merged interaction regions, and the termination shock itself. Non-compressional (Alfvénic) turbulence is driven upstream of the termination shock by the ACRs and TSPs themselves through their anisotropies.

Figure 7 shows the results of model calculations for which details of the mathematical concept are described in Zank et al. (1996b) and in Kallenbach et al. (2006). The same mixing ratio between kinetic and magnetic fluctuations as in the work by Zank et al. (1996b) has been used.

The modeled source strengths have the same scaling as in Zank et al. (1996b) and have been adapted to match observations of turbulence levels in the solar wind at 1 AU. In the upstream region of the main shock driven by the Bastille Day coronal mass ejection (Bamert et al., 2004, 2008), parallel mean free paths, acceleration time scales, Alfvén ratio, turbulence levels, cascading time scales, and energetic proton flux are consistent with theoretical predictions, in particular with the quasi-linear theory (QLT) by Lee (1983) for the energy range of protons above 60 keV. In this QLT, the protons accelerated at an interplanetary shock amplify self-consistently the upstream Alfvén waves. Analogously, anisotropic suprathermal ion flux upstream of the termination shock should amplify Alfvénic turbulence. This amplification could well make a major contribution to the reduction of the parallel mean free path in the heliosheath to about 0.5 AU as observed (Sect. 2.4) and as indicated by red color in Fig. 7. The modeled factor of 40 of increase in the Alfvénic turbulence level is based on observationally supported models on the transmission of Alfvén waves through shocks (McKenzie and Westphal, 1969; Vainio and Schlickeiser, 1999; Kallenbach et al., 2005b), which predict a factor of 4 increase in wave power spectral density at a quasi-perpendicular shock, and on an estimate of the Alfvén wave amplification factor (Lee, 1983; Bamert et al., 2004) due to anisotropic suprathermal ion flux observed upstream of the termination shock (Decker et al., 2008). However, turbulence generation by shock-generated wave-unstable conditions has to be considered as well (Fahr and Siewert, 2007, 2009).

Unfortunately, there is no published power spectral density $P(k)$ of magnetic field fluctuations in the heliosheath which would give us a direct comparison to theory on the parallel mean free path of protons, $\lambda_\parallel = 3v^2/\left[8\pi\Omega_\mathrm{p}^2 P(k)\right]$, where v is the proton speed, k the wave number, and Ω_p the angular gyro-frequency of protons in the heliosheath. However, the data by Burlaga et al. (2005) would support the increase by a factor of approximately 40. The standard deviation of magnetic field fluctuations over a fixed time interval increases by a factor 3 to 4 in the heliosheath compared to the upstream solar wind, and the convection speed of the plasma that is crossed by Voyager 2 in the heliosheath is roughly a factor 10 smaller than that of the upstream solar wind. Uncertainty remains about the exact level of Alfvénic turbulence i.e. the Alfvén ratio in the heliosheath turbulence

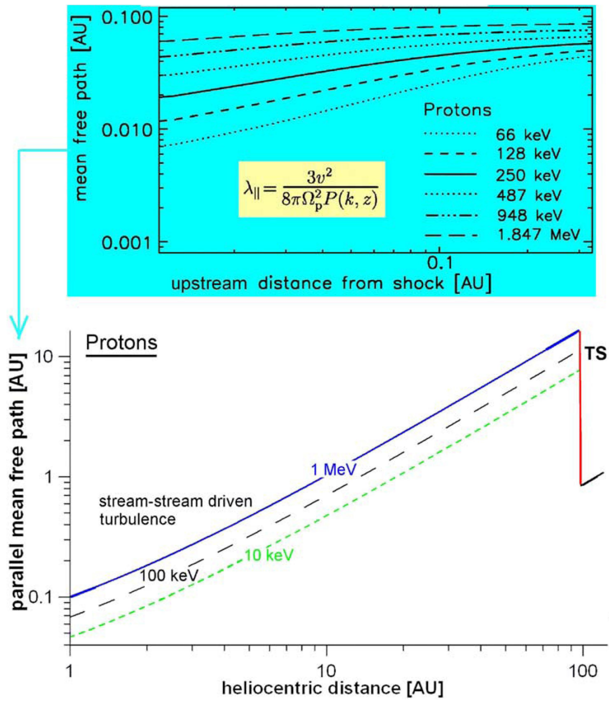

Fig. 7. (upper panel) Experimentally determined mean free paths upstream of the strongest interplanetary shock of the Bastille Day event (Bamert et al., 2004). **(lower panel)** Evolution of the parallel mean free path of protons with heliocentric distance in the ecliptic plane. The values match estimates of the parallel mean free path in the upstream region of the termination shock (2.4).

and the mixing ratio between kinetic and magnetic fluctuations. The heliosheath turbulence has a strong compressional component (Burlaga et al., 2005) probably created by the termination shock itself. This compressional component in fact is very important for stochastic acceleration of suprathermal ions i.e. the ACRs in the heliosheath.

4.2 Evolution of suprathermal ion flux with heliocentric distance

The hypothesis that ACRs are accelerated stochastically all the way through the heliosphere would be supported by the scaling of suprathermal ion flux with heliocentric distance and with energy (Fig. 8). This scaling is consistent with the evolution of compressional turbulence in the solar wind (Sect. 4.1). Details of the model are described in Kallenbach et al. (2005a); Kallenbach et al. (2006). Here, we only give a brief overview.

We solve the Parker equation written in the form

$$\frac{\partial f}{\partial t} + (\mathbf{V} + \mathbf{V}_\mathrm{D}) \cdot \nabla f = \nabla \cdot (\tilde{\kappa} \nabla f) + \frac{v}{3}\frac{\partial f}{\partial v} \nabla \cdot \mathbf{V} + \frac{1}{v^2}\frac{\partial}{\partial v}\left(v^2 D_{vv}\frac{\partial f}{\partial v}\right) + Q - S. \quad (3)$$

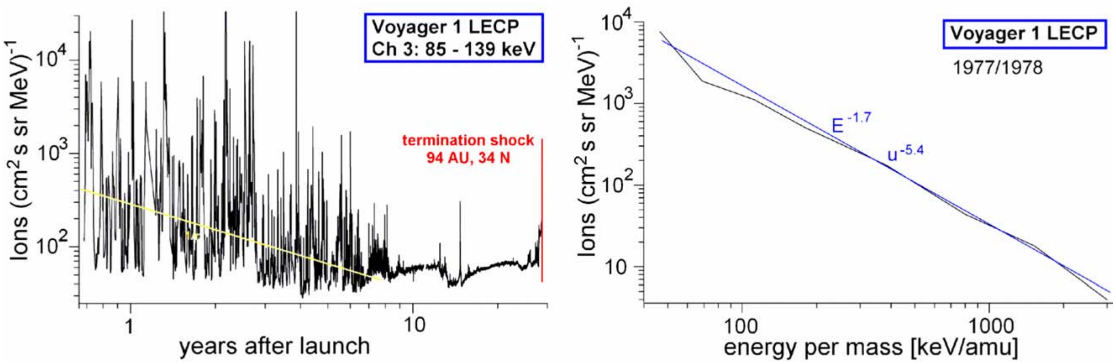

Fig. 8. The flux of suprathermal ions in average very roughly scales inversely with heliocentric distance as denoted by the yellow line (uncalibrated data of the Low Energy Charged Particle instrument from the project homepage at Caltech). A spectral index of the phase space density of 5.4 seems to be fairly typical.

The velocity **V** is the convection velocity of the bulk plasma in some reference frame such as the spacecraft frame, the tensor $\tilde{\kappa}$ describes the spatial diffusion, the parameter D_{vv} the diffusion of a nearly isotropic charged particle distribution in velocity space, and Q and S are source and sink terms such as the creation of ions in the plasma by ionization of neutrals or the reverse process, respectively. The term $(\nabla \cdot \mathbf{V})\, v \partial_v f/3$ describes the adiabatic deceleration (acceleration) in an expanding (converging) plasma flow. The velocity $\mathbf{V}_\mathrm{D}$ describes the drift of the suprathermal particles such as magnetic-field gradient or curvature drift. We neglect spatial diffusion and drift in the following. We assume spherical symmetry and constant solar wind speed, and we consider momentum diffusion in compressional turbulence regions which are larger than the mean free path for pitch-angle scattering (Bykov and Toptygin, 1981) and neglect momentum diffusion in Alfvénic turbulence. For the momentum diffusion parameter in compressional fluctuations we assume that it scales as $D_{vv} \propto r^{-1} v^2$ which is roughly consistent with the scaling used in Sect. 4.1. Any scaling law of D_{vv} close to r^{-1} may be approximated over some range of heliocentric distance by r^{-1}. Observations point towards $D_{vv} \propto r^{-0.7} v^2$ (Chalov, 2006), but the case $D_{vv} \propto r^{-1} v^2$ can be solved analytically because all terms in the Parker equation (3) resume the same power in r. This leads to an ordinary differential equation in v. The Parker equation is rewritten in speed units $u = v/V_\mathrm{SW}$ and radius $\rho = r/1\,\mathrm{AU}$. In these normalized units the momentum diffusion parameter has the form $D_2 \rho^{-1} u^2$, where D_2 is dimensionless.

We obtain a homogeneous solution f_hom from

$$-\frac{\partial f}{\partial \rho} + \frac{1}{\rho}\frac{2u}{3}\frac{\partial f}{\partial u} + \frac{D_2}{\rho}\frac{1}{u^2}\frac{\partial}{\partial u}\left[u^4 \frac{\partial f}{\partial u}\right] = 0 \;\Rightarrow$$

$$f_\mathrm{hom}(u, \rho) = f_0 \rho^{-\beta} u^{-\alpha}$$

$$\text{with } \beta = \frac{2}{3}\alpha - \alpha(\alpha - 3) D_2$$

$$\text{or } \quad \alpha \approx 3 + \frac{2}{3D_2} - \frac{3\beta}{2 + 9D_2}, \tag{4}$$

where the approximation for α applies as long as $3\beta/(2+9D_2) \ll 3 + 2/(3D_2)$.

The pre-factor f_0 and the parameter β depends on the source distribution of freshly ionized interstellar atoms $Q_\mathrm{PUI}(\mathbf{r}, v)$. This source scales as ρ^{-2} outside the ionization cavity around the Sun extending out to about 7.5 AU. For interstellar helium atoms, the ρ^{-2} scaling is valid further inwards, in particular in the upwind direction of the interstellar medium, i.e. $Q(u, \rho) = \rho^{-2} q(u)$ for $\rho > 1$. The inhomogeneous solution f_inhom then scales as ρ^{-1} i.e. $\beta = 1$.

Trusting the simplified model, typical values of D_2 can be derived from the observed spectral index of suprathermal tails. They are in the range $\alpha \approx 5...6$ (Gloeckler, 2003). For a momentum diffusion parameter $D_2 \approx 0.2$ (and $\beta = 1$) the spectral index is $\alpha \approx 5.4$. The quantity $D_2 \approx 0.2$ is consistent with the modeled turbulence levels (Sect. 4.1). Note that the spectral index α cannot be smaller than 5. This is the limit, when stochastic acceleration becomes the dominant term in the transport equation, i.e. $D_2 > 1$. In that case, the quasi-linear description breaks down and one gets a cascade in speed represented by a phase space density scaling as v^{-5} (Fisk and Gloeckler, 2008).

Note, however, that power-law pick-up ion tails extending to high energies may cause a very high suprathermal-ion pressure in the termination shock region. Fahr (2007) has shown that this pressure could lead to effective Mach numbers below unity at the termination shock. Naturally, the v^{-5} power law breaks down at some maximum speed v_max given, for instance, by the equality of the scattering mean free path and the outer scale of the compressional turbulence. The phase space densities used in the models by Kallenbach et al. (2005a); Kallenbach et al. (2006) imply a suprathermal-ion pressure which is small compared to the dynamic pressure of the bulk solar wind upstream of the termination shock. A typical phase space density is characterized by the parameter $f_0 \approx 50\,\mathrm{s}^3\,\mathrm{m}^{-6}$ in Eq. (4) (see also caption of Fig. 10). In fact, the parameter f_0 not only depends on the strength of the shell-like source distribution of freshly ionized interstellar atoms $Q_{\mathrm{PUI}}(\mathbf{r}, v)$ (Vasyliunas and Siscoe, 1976), but also depends on how fast pick-up ions are injected from this shell distribution into the power-law distributions. This is another type of 'injection problem'.

4.3 Acceleration time scales in the heliosheath

The hypothesis that ACRs are accelerated stochastically in the heliosheath is also supported by an estimate of the acceleration time scales. Stochastic acceleration in compressional fluctuations has a shorter time scale than first-order Fermi acceleration down to ion energies below 100 keV/amu. This again is based on the previously mentioned turbulence models (Sect. 4.1) which are supported by observations.

For mathematical details of the comparison of the acceleration time scales for first-order Fermi acceleration at the termination shock with stochastic acceleration (second-order Fermi) in the heliosheath we refer to Kallenbach et al. (2005a); Kallenbach et al. (2006) and references therein. The time scale for first-order Fermi acceleration is:

$$t_{\mathrm{acc}} = \frac{3}{V_{\mathrm{up}} - V_{\mathrm{ds}}} \int_{v_0}^{v_1} \left(\frac{v \Lambda_{\mathrm{r;up}}}{3 V_{\mathrm{up}}} + \frac{v \Lambda_{\mathrm{r;ds}}}{3 V_{\mathrm{ds}}} \right) \frac{\mathrm{d}v}{v} \quad \Rightarrow$$

$$\tau_{\mathrm{acc;F1}} := \frac{\mathrm{d}t_{\mathrm{acc}}}{\mathrm{d}v} v \approx \left(\frac{E}{1\mathrm{MeV}} \right)^{2/3} \cos^2 \Psi \left(\frac{A}{Q} \right)^{1/3} \mathrm{yr}\,, \qquad (5)$$

For this rough estimate, turbulence levels are assumed that are consistent with observed mean free paths of order 0.5 AU for protons with 1 MeV energy (Sect. 2.4).

Compared to this, the acceleration time scale for stochastic acceleration in compressional fluctuations in the upstream slow solar wind with $D_2 \approx 0.2$ is about 4 years. This is derived with $\rho \approx 100$ from Eq. (4), which is written in units of the solar wind convection time scale near Earth. If the compressional fluctuations are stronger by a factor 40 in the heliosheath compared to the upstream solar wind, the acceleration time scale may be about 0.1 year at any energy and mass-per-charge ratio of the ions. This shows that in particular at the high energies stochastic acceleration may well compete with first-order Fermi acceleration.

4.4 ACR injection source distributions

Note that only in the slow solar wind is the momentum diffusion parameter as large as $D_2 \approx 0.2$, while the fast solar wind has mainly Alfvénic fluctuations, and D_2 is much smaller. If the main injection source for ACRs are pick-up ions which are stochastically pre-accelerated in the upstream solar wind, then this source is generally stronger in the ecliptic plane during solar activity minimum. During solar activity maximum, slow streams are more evenly distributed all over the heliosphere. This source distribution of pick-up ions is in fact not much different when compared to the alternative scenario where first-order Fermi acceleration is the dominant ACR acceleration process. Scherer and Fahr (2009) model injection into the ACR regime from a three-dimensional termination shock surface where the shock-normal angle of the termination shock is decisive for efficient injection. They find, that during solar activity minimum, injection is most efficient near the ecliptic plane. However, in their scenario injection is much more efficient at the flanks of the heliosphere rather than at the apex and anti-apex. However, observations suggest increased ACR intensities near the apex and antiapex of the heliosphere during solar activity minimum (Hilchenbach et al., 1998). Data from the Interstellar Boundary Explorer mission (McComas et al., 2009) may resolve some of these open issues.

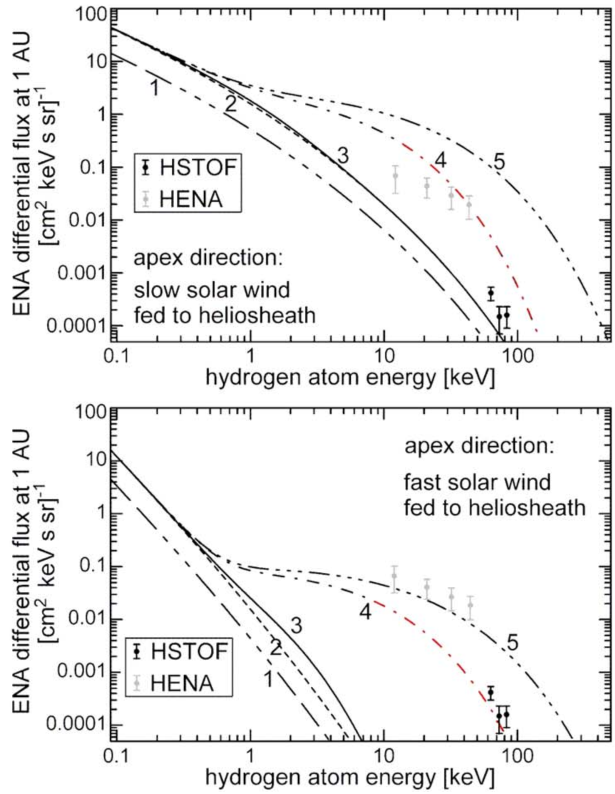

Fig. 9. Predicted spectra of suprathermal protons through stochastic acceleration by Alfvénic turbulence in the heliosheath as observable in energetic neutral atoms (ENAs) at 1 AU and comparison to data of the CELIAS/HSTOF sensor onboard the SOHO spacecraft and to upper limits derived by the HENA sensor onboard the IMAGE spacecraft. The red-marked curves are the predictions that correspond to Alfvénic turbulence levels resulting from observed anisotropic TSP flux.

In support of the hypothesis of stochastic acceleration being an important process, we would like to emphasize here that in the energy range between solar wind energies and a few tens of keV/amu, even Alfvénic fluctuations in the heliosheath are sufficient for stochastic acceleration. Figure 9 shows the predicted flux spectra of energetic neutral hydrogen atoms (EHAs) near Earth's orbit resulting from stochastic acceleration of suprathermal protons in Alfvénic turbu-

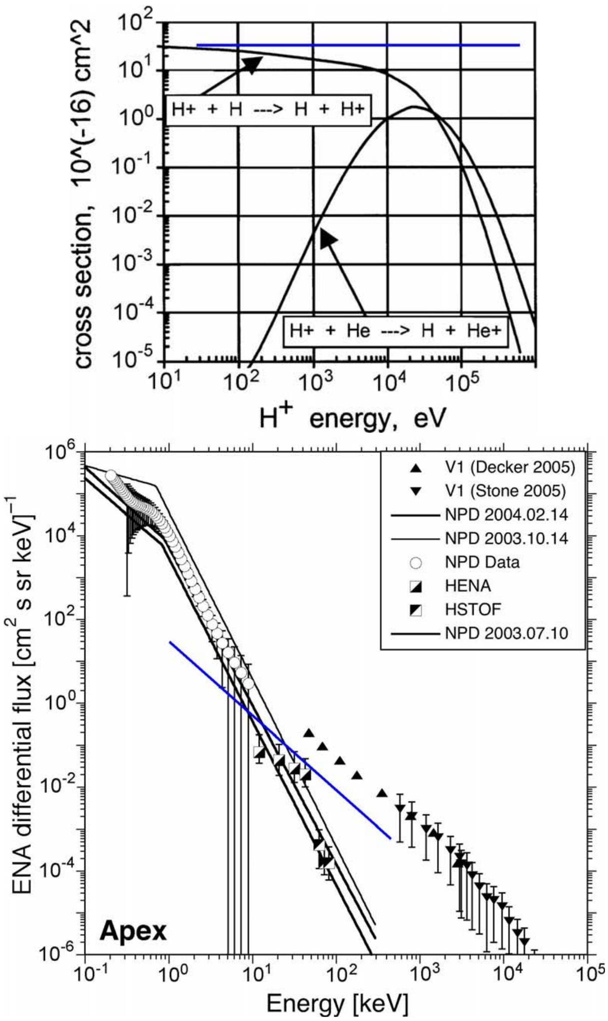

Fig. 10. Voyager 1 in-situ ion flux data (Stone et al., 2005) from the heliosheath plasma and "remote-sensing" energetic neutral atom data from CELIAS/HSTOF (Kallenbach et al., 2006), HENA IMAGE data (E. Roelof, private communication), and Mars Aspera-3 NPD data (Galli et al., 2006). The blue line indicates the model proton spectra in the heliosheath for the injection of the minimum flux of suprathermal tails in the slow solar wind $f = f_0 \rho^{-1} u^{-5}$, $f_0\,(u=1) \approx 50\,\mathrm{s}^3\,\mathrm{m}^{-6}$ (Gloeckler, 2003), and an enhancement of their flux by about a factor 10 at the termination shock. That HSTOF data are below the blue line is due to the fact that the charge exchange cross section decreases at higher energies, as is illustrated in the upper panel (Gruntman et al., 2001).

lence in the heliosheath. The predictions that correspond to Alfvénic turbulence levels resulting from wave amplification through anisotropic TSP flux at the level observed by Voyager indeed match observations of EHAs at 1 AU by CELIAS/HSTOF onboard SOHO.

The modeled spectra of Fig. 9 could perhaps even explain the spectral index of -1.25 observed by Decker et al. (2008) which is even harder than the -1.5 for the ubiquitous suprathermal tails (Gloeckler, 2003).

4.5 Observed ACR and energetic neutral atom spectra

Until December 2004, only energetic neutral atom (ENA) observations for H and He by CELIAS/HSTOF were available to analyze suprathermal ion flux data in the heliosheath. The flux of ENAs near Earth's orbit created from the suprathermal ion tails anywhere in the heliosphere is modeled in detail by Gruntman et al. (2001), Kallenbach et al. (2005a), and Kallenbach et al. (2006). Since the crossing of the termination shock by Voyager 1 (Stone et al., 2005) in December 2004, there are in-situ measurements of suprathermal ion distributions in the heliosheath plasma. Figure 10 demonstrates that estimates of the suprathermal ion flux in the heliosheath from CELIAS/HSTOF data are roughly in agreement with the in-situ measurements.

Some new data have been contributed by the Neutral Particle Detector (NPD) onboard Mars Express. At low energies ($< 10\,\mathrm{keV}$), the phase space densities of hydrogen atoms are definitely higher than the values derived from preacceleration in the supersonic solar wind and further acceleration in the heliosheath. This indicates that further injection into stochastic acceleration of low-energy protons takes place in the heliosheath. In fact, this process appears to be very efficient. The high levels of compressional fluctuations observed in the heliosheath (Burlaga et al., 2005) support this view.

5 Conclusions

Turbulence and ion acceleration are intimately linked processes of the outer heliosphere. The analysis of this article supports the idea that stochastic acceleration in compressional fluctuations in the heliosheath is a process that can compete with first-order Fermi acceleration at the solar wind termination shock. A viable explanation for the composition of termination shock energetic particles (TSPs) and anomalous cosmic rays (ACRs) is that TSPs are particles which are reflected as slightly suprathermal ions at the electric cross-shock potential of the solar wind termination shock and subsequently accelerated by the first-order Fermi process, while ACRs are particles transmitted as slightly suprathermal ions through the electric cross-shock potential of the termination shock and subsequently stochastically accelerated in the compressional fluctuations of the heliosheath. Probably, the two processes of first-order Fermi acceleration and second-order Fermi acceleration are intertwined. Particles that are stochastically accelerated in the heliosheath may eventually reach an energy which gives them a sufficiently large mean free path to cross the termination shock again to participate in first-order Fermi acceleration. The relative importance of first-order and second-order Fermi acceleration in different energy ranges, at different heliolongitudes and heliolatitudes, and during different solar activity phases still remains to be evaluated quantitatively from past and future observations.

Lessons may be learned from the heliosphere for galactic acceleration processes. Second-order Fermi acceleration may also be responsible for the energization of the Galactic Cosmic Rays (GCRs). Warren et al. (2005) have observed that the turbulence region downstream of the blast wave of the Tycho supernova is thinner than magnetohydrodynamic models predict. This may be analogous with the reduced size of the heliosheath due to the ACR pressure there. As the sum of the ACR pressure and the heliosheath bulk pressure balances the pressure of the interstellar medium, the heliosheath bulk pressure is reduced in the presence of the ACRs and the size of the heliosheath is consequently reduced.

This has been taken as an argument for the presence of GCRs in the region between the blast wave and the contact discontinuity of the bubble of the Tycho supernova. In fact, it has been taken as evidence that a supernova shock wave accelerates the GCRs. This result may have to be verified. It may actually be the turbulence downstream of the supernova shock that accelerates the GCRs.

Acknowledgements. The authors very much thank the two anonymous referees for very helpful suggestions. Many thanks go to the International Space Science Institute (ISSI) in Bern for hosting the second International Heliophysical Year Conference and to the convenors of this conference, in particular to H.-J. Fahr.

The service charges for this open access publication
have been covered by the Max Planck Society.

Edited by: K. Scherer
Reviewed by: two anonymous referees

References

Alexashov, D. B., Chalov, S. V., Myasnikov, A. V., Izmodenov, V. V., and Kallenbach, R.: The dynamical role of anomalous cosmic rays in the outer heliosphere, Astron. Astrophys., 420, 729–736, 2004.

Bamert, K., Kallenbach, R., Ness, N. F., Smith, C. W., Terasawa, T., Hilchenbach, M., Wimmer-Schweingruber, R. F., and Klecker, B.: Hydromagnetic wave excitation upstream of an interplanetary traveling shock, Astrophys. J., 601, L99–L102, 2004.

Bamert, K., Kallenbach, R., le Roux, J. A., Hilchenbach, M., Smith, C. W., and Wurz, P.: Evidence for Iroshnikov-Kraichnan-type turbulence in the solar wind upstream of interplanetary traveling shocks, Astrophys. J., 675, L45–L48, 2008.

Baumjohann, W., and Treumann, R. A.: Basic Space Plasma Physics, Imperial College Press, London, 1996.

Burlaga, L. F., Ness, N. F., Acuña, M. H., Lepping, R. P., Connerney, J. E. P., Stone, E. C., and McDonald, F. B.: Crossing the termination shock into the heliosheath: magnetic fields, Science, 309, 2027–2029, 2005.

Burlaga, L. F., Ness, N. F., Acuña, M. H., Lepping, R. P., Connerney, J. E. P., and Richardson, J. D.: fields at the solar wind termination shock, Nature, 454, 75–77, 2008.

Bykov, A. M. and Toptygin, I. N.: Phys.-Uspekhi, 36, 1020, 1993.

Chalov, S. V. and Fahr, H.-J.: Pick-up ion acceleration at the termination shock and the post-shock pick-up ion energy distribution, Astron. Astrophys., 360, 381–390, 2000.

Chalov, S.: Interstellar pickup ions and injection problem for Anomalous Cosmic Rays: Theoretical aspect, in: The Physics of the Heliospheric Boundaries, edited by V. V. Izmodenov and R. Kallenbach, ESA Publications Division, ESTEC, The Netherlands, November, 2006, ISBN 1608-280X, 245, 2006.

Decker, R. B., Krimigis, S. M., Roelof, E. C., Hill, M. E., Armstrong, T. P., Gloeckler, G., Hamilton, D. C., and Lanzerotti, L. J.: Mediation of the solar wind termination shock by non-thermal ions, Nature, 454, 67–70, 2008.

Fahr, H.-J.: Global energy transfer from pick-up ions to solar wind protons, Sol. Phys., 208, 335–344, 2002.

Fahr, H.-J.: Revisiting the theory of the evolution of pick-up ion distributions: magnetic or adiabatic cooling?, Ann. Geophys., 25, 2649–2659, 2007.

Fahr, H.-J. and Siewert, M.: Anisotropic unstable ion distribution functions downstream of the solar wind termination shock, Astrophys. Space Sci. Trans., 3, 21, 2007.

Fahr, H.-J. and Chalov, S. V.: Supersonic solar wind ion flows downstream of the termination shock explained by a two-fluid shock model, Astron. Astrophys., 490, L35–L38, 2008.

Fahr, H.-J. and Siewert, M.: Pressure anisotropies mapped through the solar Wind termination shock, Astrophys. J., 693, 281–284, 2009.

Fahr, H.-J. and Verscharen, D.: Ion reflections from the parallel MHD termination shock and a possible injection mechanism into the Fermi-1 acceleration, Astron. Astrophys., 487, L21–L24, 2008.

Fahr, H.-J., Scherer, K., Potgieter, M. S., Ferreira, S. E. S.: Longitudinal variation of the pickup-proton-injection efficiency and rate at the heliospheric termination shock, Astron. Astrophys., 486, L1–L4, 2008.

Ferreira, S. E. S., Potgieter, M. S., and Scherer, K.: The transport and acceleration of anomalous cosmic rays in the inner heliosheath, J. Geophys. Res., 112, A11101, 2007.

Fisk, L. A., Kozlovsky, B., and Ramaty, R.: An interpretation of the observed oxygen and nitrogen enhancements in low-energy cosmic rays, Astrophys. J., 190, L35, 1974.

Fisk, L. A. and Gloeckler, G.: Acceleration of suprathermal tails in the solar wind, Astrophys. J., 686, 1466–1473, 2008.

Galli, A., et al.: Direct measurements of energetic neutral hydrogen in the interplanetary medium, Astrophys. J., 644, 1317–1325, 2006.

Giacalone, J. and Jokipii, J. R.: The transport of cosmic rays across a turbulent magnetic field, Astrophys. J., 520, 204–214, 1999.

Gloeckler, G.: Ubiquitous suprathermal tails on the solar wind and pickup ion distributions, Solar Wind 10, AIP Conf. Proc., 679, 583–588, 2003.

Gruntman, M., Roelof, E. C., Mitchell, D. G., Fahr, H.-J., Funsten, H. O., and McComas, D. J.: Energetic neutral atom imaging of the heliospheric boundary region, J. Geophys. Res., 106, 15 767–15 782, 2001.

Hilchenbach, M., Hsieh, K. C., Hovestadt, D., et al.: Detection of 55–80 keV hydrogen atoms of heliospheric origin by CELIAS/HSTOF on SOHO, Astrophys. J., 503, 916–922, 1998.

Kallenbach, R., Hilchenbach, M., Chalov, S. V., Le Roux, J. A., and Bamert, K.: On the injection problem at the solar wind termina-

tion shock, Astron. Astrophys., 439, 1–22, 2005a.
Kallenbach, R., Bamert, K., Hilchenbach, M., and Smith, C. W.: Observations of turbulence near interplanetary travelling shocks, in: The Physics of Collisionless Shocks, AIP Conf. Proc., 781, 129–134, 2005b.
Kallenbach, R., Czechowski, A., Hilchenbach, M., and Wurz, P.: Turbulence and ion acceleration in the outer heliosphere, in: The Physics of the Heliospheric Boundaries, edited by V. V. Izmodenov and R. Kallenbach, ESA Publications Division, ESTEC, The Netherlands, November, 2006, ISBN 1608-280X, 203, 2006.
Lee, M. A.: Coupled hydromagnetic wave excitation and ion acceleration at interplanetary traveling shocks, J. Geophys. Res., 88, 6109–6119, 1983.
Lee, M. A.: The injection, acceleration, and dynamical influence of interstellar pickup ions at the solar wind termination shock, Astrophys. Space Sci., 264, 497–508, 1998.
Lee, M. A., Shapiro, V. D., and Sagdeev, R. Z.: Pickup ion energization by shock surfing, J. Geophys. Res., 101, 4777–4790, 1996.
Lee, M. A., Fahr, H.-J., Kucharek, H., Moebius, E., Prested, C., Schwadron, N. A., and Wu, P.: Physical processes in the outer heliosphere, Space Sci. Rev., DOI 10.1007/s11214-009-9522-9, 2009.
Lembège, B. and Savoini, P.: Nonstationarity of a two-dimensional quasiperpendicular supercritical collisionless shock by self-reformation, Phys. Fluids, B4, 3533–3548, 1992.
le Roux, J. A., Fichtner, H., and Zank, G. P.: Self-consistent acceleration of multiply reflected pickup ions at a quasi-perpendicular solar wind termination shock: a fluid approach, J. Geophys. Res., 105, 12 557–12 578, 2000.
Matsukiyo, S. and Scholer, M.: Modified two-stream instability in the foot of high Mach number quasi-perpendicular shocks, J. Geophys. Res., 108, SMP 19-1, CiteID 1459, DOI 10.1029/2003JA010080, 2003.
McComas, D. J. and Schwadron, N. A.: An explanation of the Voyager paradox: Particle acceleration at a blunt termination shock, Geophys. Res. Lett., 33, CiteID L04102, 2006.
McComas, D. J., Allegrini, F., Bochsler, P., et al.: IBEX Interstellar Boundary Explorer, Space Sci. Rev., in press.
McKenzie, J. F. and Westphal, K. O.: Transmission of Alfvén waves through the Earth's bow shock, Planet. Space Sci., 17, 1029–1037, 1969.
Moraal, H., Caballero-Lopez, R. A., McCracken, K. G., McDonald, F. B., et al.: Cosmic ray energy changes at the termination shock and in the heliosheath, AIP Conf. Proc., 858, 219, 2006.
Richardson, J. D., Kasper, J. C., Wang, C., Belcher, J. W., and Lazarus, A. J.: Cool heliosheath plasma and deceleration of the upstream solar wind at the termination shock, Nature, 454, 63–66, 2008.
Sagdeev, R. Z.: Cooperative phenomena and shock waves in collisionless plasmas, in: Reviews of Plasma Physics, edited by M. A. Leotovich, 4, Consultants Bur., New York, 23, 1966.
Scherer, K. and Fahr, H.-J.: Spatial variation of the pickup-proton-injection rate into the ACR regime at the 3D-heliospheric termination shock, Astron. Astrophys., 495, 631–638, 2009.
Scholer, M., Shinohara, I., and Matsukiyo, S.: Quasi-perpendicular shocks: Length scale of the cross-shock potential, shock reformation, and implication for shock surfing, J. Geophys. Res., 108, 1014, doi:10.1029/2002JA009515, 2003.
Stone, E. C., Cummings, A. C., McDonald, F. B., Heikkila, B. C., Lal, N., and Webber, W. R.: Voyager 1 explores the termination shock region and the heliosheath beyond, Science, 309, 2017–2020, 2005.
Tidman, D. A. and Krall, N. A.: Shock waves in collisionless Plasmas, in: Series in Plasma Physics, edited by S. C. Brown, Wiley, New York, 29–38, 1971.
Vainio, R. and Schlickeiser, R.: Self-consistent Alfvén-wave transmission and test-particle acceleration at parallel shocks, Astron. Astrophys., 343, 303–311, 1999.
Vasyliunas, V. M. and Siscoe, G. L.: On the flux and the energy spectrum of interstellar ions in the solar system, J. Geophys. Res., 81, 1247–1252, 1976.
Verscharen, D. and Fahr, H.-J.: A kinetic description of the dissipative quasi-parallel solar wind termination shock, Astron. Astrophys., 487, 723–729, 2008.
Warren, J. S., Hughes, J. P., Badenes, C., Ghavamian, P., McKee, C. F., Moffett, D., Plucinsky, P. P., Rakowski, C., Reynoso, E., and Slane, P.: Cosmic-ray acceleration at the forward shock in Tycho's supernova remnant: evidence from Chandra X-ray observations, Astrophys. J., 634, 376–389, 2005.
Zank, G. P., Pauls, H. L., Cairns, I. H., and Webb, G. M.: Interstellar pickup ions and quasi-perpendicular shocks: Implications for the termination shock, J. Geophys. Res., 101, 457–478, 1996a.
Zank, G. P., Matthaeus, W. H., and Smith, C. W.: Evolution of turbulent magnetic fluctuation power with heliospheric distance, J. Geophys. Res., 101, 17 093–17 107, 1996b.
Zank, G. P., Li, G., Florinski, V., Hu, Q., Lario, D., and Smith, C. W.: Particle acceleration at perpendicular shock waves: Model and observations, J. Geophys. Res., 111, CiteID A06108, 2006.
Zhang, M.: Acceleration of galactic and anomalous cosmic rays in the heliosheath, AIP Conf. Proc., 858, 226, 2006.